Direct observation of carbon nanostructures growth using in-situ ultrahigh vacuum transmission electron microscopy

Y. L. Foo,[1,*] M. Lin,[1] J. P. Y. Tan,[1] C. B. Boothroyd,[1] E. S. Tok[2]

[1]Institute of Materials Research and Engineering, 3 Research Link S117602, Singapore
[2] Department of Physics, National University of Singapore, 2 Science Drive 2, S117542
[*]yl-foo@imre.a-star.edu.sg

ABSTRACT

We report the growth dynamics of a single-walled carbon nanotube (SWNT) using an in situ ultrahigh vacuum transmission electron microscope at 650 °C. SWNTs preferentially grow on smaller sized catalyst particles (diameter < 6 nm) with three distinct growth regimes (incubation, growth, and passivation). All of the observed SWNTs grow via a base-growth mechanism with C diffusion on active Ni catalyst sites. Under the same experimental conditions, formation of carbon nanocages was observed on larger Ni catalyst particles. The evolution of SWNTs or nanocages is dependent on catalyst size, and this can be rationalized from both energetics and kinetics considerations. The real time observation of bamboo-like carbon nanotube will be addressed during the talk.

Keywords: carbon, nanostructure, mechanism

1 INTRODUCTION

Carbon based nanostructures can be grown by arc discharge, laser ablation and chemical vapor deposition (CVD). Amongst them, CVD is the most attractive candidate for industrial adoption due to its scalability and low cost. Most CNT formation mechanisms have been studied by theoretical calculations *(1-3)* or post-deposition high-resolution transmission electron microscopy (TEM) *(4-11)*. Often, CVD growth using same experimental growth condition yields 'different' types of structures (e.g. SWNT, double-walled nanotubes (DWNT), multi-walled nanotubes (MWNT), sheets, cages and amorphous tubes) *(12-16)*, making complete and detailed understanding of reactions difficult. This is further aggravated by the ambient/low vacuum growth conditions that convolute data with contaminants. There is a long-standing controversy in the mechanism of carbon nanostructures growth by CVD method. Baker and co-workers proposed that the hydrocarbon decomposes on surface of metal particles to form carbon adsorbates. The carbon adatom then diffuse through the bulk of the metal, driven by concentration gradient, before precipitating in form of graphite on a different surface of the catalytic particle. De Bokx et al contradict this theory and proposed that catalyst is converted intermediate carbides during growth before decomposing to graphene layers.*(17,18)* There is, however, no validation of either mechanism due to absence of experimental proof on the structure of catalyst at steady state during growth at elevated temperature. All previous studies by TEM are carried out after growth, under ambient condition, where the structure of catalyst could have undergone phase transition, to a phase entirely different from steady state growth.

At present there is no concerted effort to correlate the type of carbon nanostructure (single, double or multi-walled tubes, sheets, cages or onions) to growth temperature, flux and catalyst *in situ*. The *in-situ* ultra-high vacuum (UHV) TEM operating in both direct and reciprocal space, is thus an ideal platform for conducting these experiments due to its capability for real time observation on the nanometer scale. This enables quantitative investigation of the reaction pathways and growth kinetics of carbon nanostructures at elevated temperatures to be possible.

2 EXPERIMENT & DISCUSSION

NiO-MgO precursors were prepared by co-precipitation of $Ni(NO_3)_2$ and $Mg(NO_3)_2$ mixture solutions at a molar ratio of 1:1. The obtained precipitates were dried at 100 °C, ground into powders, calcined in air at 700 °C for 2 hours to decompose the nitrites, and reduced in H_2 atmosphere at 700 °C for 2 hours to form reactive Ni nanoparticles on the MgO substrate. Our technique of catalyst preparation results in Ni particles with different sizes distribution on the support MgO substrates. This allows us to study the effects of catalyst particle size in parallel in a *single* experiment, with *all* other experimental conditions remaining constant. Therefore, we can make direct comparison of effect of shape, size, and morphology of catalyst on resultant types of carbon nanostructure grown. The reactively fresh Ni-MgO catalysts were ultrasonically dispersed in absolute ethanol and then cast on a holey carbon coated Mo grid that

was then mounted over a Si heating piece. The *in-situ* TEM equipped with an atomic hydrogen cracker source, was used to activate the catalysts through reduction of surface oxides. Acetylene (C_2H_2) was passed into the TEM column through a leak valve, the microscope has a backfilled pressure of ~4×10^{-6} Torr during reaction and the temperature of the catalysts was maintained at 650 °C. Growth of SWNT and carbon nanostrutures is captured using both the Gatan DV300 and GIF2000 image acquisition system.

Our catalyst preparation technique through wet chemistry yields Ni with high dispersity in diameters. This enables us to study the effect of catalyst dimension within a single experiment, with all other experimental conditions remaining constant, in the in-situ UHVTEM. We can, therefore, make direct inference of effect of size and morphology of catalyst on type carbon nanostructure grown. During growth at T = 650 °C and $P_{C2H2} = 4\times10^{-6}$ Torr, we observed SWNTs and nanocages formation. Fig. 1a and b are HRTEM image showing typical SWNTs and nanocages respectively. Our TEM images show that all the SWNT tips are closed and there are no catalyst particles at the tips, indicating all the SWNTs follow base-growth mechanism. The effect of catalyst dimension on types of carbon structures formation is illustrated on a histogram as shown in Fig 1c. Under our experimental condition, the smaller Ni catalyst (diameters < 6 nm) favors formation of SWNTs whilst larger catalyst prefers nanocages formation. Fig. 1d is a plot of SWNT tube diameter vs catalyst size. Regression analysis indicates the diameter ratio between nanotubes and Ni particles ~ 1.2. This insight developed through the in-situ TEM experiment, clearly suggests that we can therefore, grows large array SWNTs with controlled diameter for technological application through engineering monodisperse nanoscale catalyst.

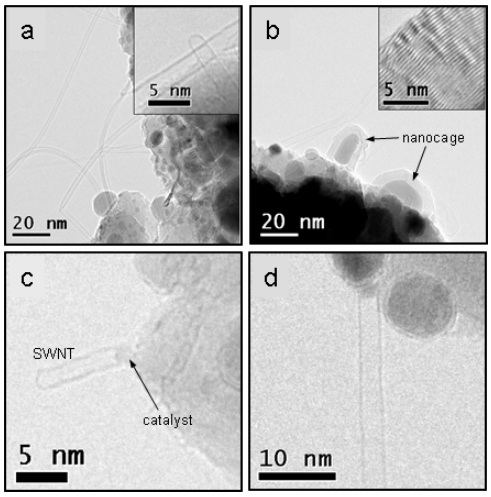

Figure 1: SWNT and Nanocage growth. SWNT prefers to grow on smaller catalyst while cages grow on larger catalyst (> 6nm)

We used electron diffraction patterns (DP) to follow the crystal structure of catalyst both before and during growth at 650 °C. Fig. 2a is the DP of the Ni-MgO catalyst before C_2H_2 dosing while Fig. 2b is the DP of Ni-MgO during steady state growth. Both DPs comprise of Ni and MgO diffraction rings, indicating that the catalyst particles remain as metallic Ni during growth. The absence of Ni_3C in DPs strongly suggest that de Bokx et. al. model, where carbides are formed prior to precipitation to carbon nanostructure, is not the operative mechanism during growth of SWNTs and nanocages. The more plausible mechanism for growth is either through surface or bulk diffusion of C atoms on or in metallic Ni catalyst respectively.

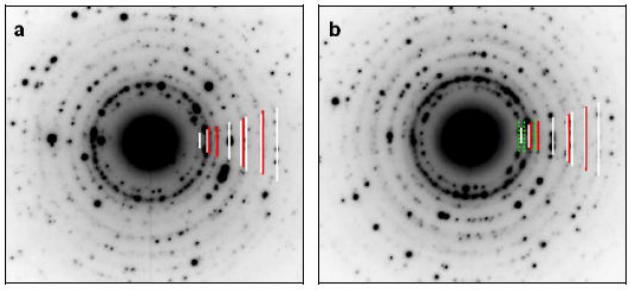

Fig. 2 Diffraction pattern of Ni catalyst at 650 °C (a) before (b) during C_2H_2 dosing

First principle calculations shows an extended graphene layer on catalyst is more stable than an aggregate of isolated carbon atoms on Ni surface. The difference in free energy thus provides the driving force for the hemispherical carbon cap formation during the initial growth stages. At elevated temperature, incoming C adatoms from catalytic decomposition will re-arrange the graphite ring/catalyst growth boundary into a more energetically favorable configuration system through surface diffusion and coalescence. There are two plausible diffusion pathways for C in/on Ni catalyst during SWNT growth namely, bulk diffusion and/or surface diffusion, to the boundary of the growth interface (i.e Ni and CNT basal ring). The latter has lower activation barriers due to lesser coordination. Our experimental results show that Ni catalyst, as depicted in Fig. 1, with small diameter (< 6 nm) favors SWNTs growth whilst larger catalyst favors nanocages formation. There appears to be a size selection of catalyst in determining the type of final products. The growth of these graphene layers resulting in either the formation of a closed tip SWNT with a hemispherical graphene carbon cap or a graphene sphere-carbon nanocages therefore suggest the initial nucleation

NSTI-Nanotech 2007, www.nsti.org, ISBN 1420061828 Vol. 1, 2007

dynamics of these features depends on the size of the catalyst. The development of a hemispherical graphene cap (precursor to formation of a closed SWNT tip) or a graphene sphere (precursor to formation of nanocage) is driven by the need to minimize the energy associated with nucleation of the graphene layer when constrained to grow and form a nanotube or a nanocage, in particular, the interplay between the surface energy and strain energy per unit volume on a small or large catalyst. A larger catalyst particle possesses lower curvature than that of a smaller catalyst particle and this allows formation of a graphene sphere that envelopes the catalyst particle with lower strain energy because the torsional stress on the C-C bond within the graphene sheet is smaller. The torsional stress within the graphene layers will increase with decreasing dimensions of the catalyst particle and the build up in strain energy will dominate the total energy, thus making the graphene sphere formation unlikely for small catalyst particles. Instead, a partial ring develops and in this instance a hemispherical graphene cap is formed. The built up strain energy is relaxed by allowing tubular growth with the cap as the tip. This is analogous to the island shape transitions observed in strain layer epitaxy where a symmetric shaped island grows to from a wire *(19)*.

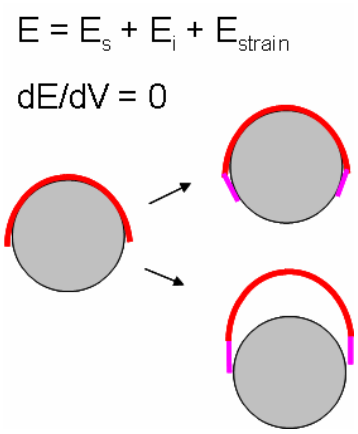

Fig. 3 Critical catalyst size for transition in growth mode.

Thus as more carbon atoms are added, the SWNT wall forms and lengthens. This growth model is likened to the yarmulke mechanism *(20)*. This strain relaxation effect in SWNT growth is also augmented by the fact that on a smaller catalyst, bulk diffusion can become significant (the diffusion length is comparable to the catalyst diameter) and the catalytic activity for decomposition is higher, thus leading to higher apparent local adatom density for growth.

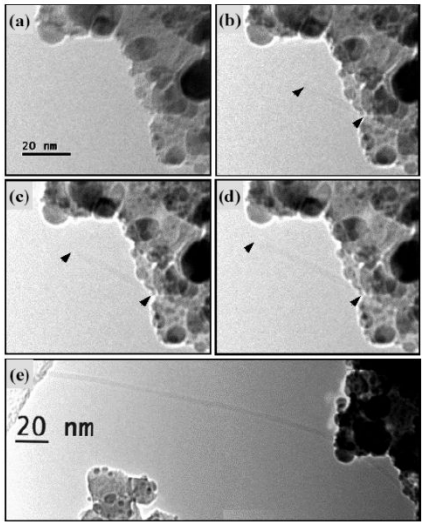

Fig. 4 BF image of SWNT as function of time

To get an insight into the dynamical growth of SWNTs, a sequence of bright field (BF) images was used to follow the growth process of a single SWNT. *(21)* Fig. 3a is the BF image of Ni catalyst at t = 0s. As the C_2H_2 doser is opened, we observed the growth process of an SWNT with diameter ~ 3.3 nm, as shown in Fig 4b-d, on a 4 nm Ni catalyst. The absence of kinks on SWNT and its constant diameter suggest the SWNT has low defect density. Although the thermal vibration of the unsupported extended segment makes the images slightly unclear at 650 ^{o}C, we are still able to measure its length as function of growth time and hence estimate its growth rate.

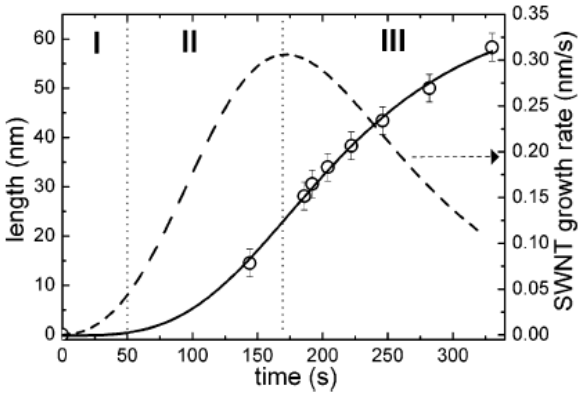

Fig. 5 is the plot of length and growth rate vs reaction time.

The growth rate, initially at 3.3 Å/s, tails down to 1.7 Å/s after t > 200 s. To the first approximation, ~ 250 carbon atoms were incorporated into the nanotube per second,

during the initial growth rate of 3.2 Å/s. The growth of the SWNT appears to have three distinct regimes under the present growth conditions. There is a slow growth rate region at t < 20 s (Regime I), followed by a rapid increase in growth rate (Regime II) up to t = 170 s, before a regime where the grow rates decay with increasing reaction time (Regime III). The growth rate of SWNT can be expressed as RSWNT = k $[P_{C2H2}]m$ [θ]n, where k is the rate constant, P_{C2H2} is the pressure of C_2H_2 and θ is the surface coverage of active surface site on Ni catalyst. At t = 0s, the surface coverage of active sites θ =1 and backfilled pressure P_{C2H2} ~ 4×10^{-6} Torr. Regime I on the growth rate diagram is analogous to the incubation/critical nuclei formation period in crystal growth whereby the thermally activated Ni catalyst/SWNT ring and the SWNT hemispherical cap on the surface of the catalyst are formed. The interpolated length of SWNT is < 1 nm in regime I. This is followed by a rapid growth regime where the SWNT length increases. In Regime II, the growth rate increases from RSWNT = 0.008 nm/s at t = 20 s to RSWNT(max) = 0.31 nm/s at t = 173 s. At the maximum growth rate, ~ 250 carbon atoms were incorporated into the SWNT per second. The increase in growth rate is likely due to the increase in C adatom density on the surface of the N catalyst, thereby increasing the C atoms flux attaching to the SWNT ring/catalyst growth front. In regime III, we observed decay in the growth rate. Since all parameters experimental (temperature, P_{C2H2}) condition remains constant, the reduction in growth rate is likely to be cause by catalyst poisoning, thereby reducing its efficiency. Due to the surface diffusion of carbon atoms during the SWNT growth process, some deactivated carbon atoms that are adsorbed strongly on the surface will block carbon diffusion, consequently rendering the other carbon atoms inactive towards continued SWNT growth. This phenomena was reported previously and successfully overcome by addition of water vapor in the feed gas, which acts as weak oxidizer, to remove some strongly adsorbed carbon atoms and maintain activity of catalysts.

3 ACKNOWLEDGMENT

The authors acknowledge the financial support from the Institute of Materials Research and Engineering (IMRE), and the Department of Physics at national University of Singapore.

REFERENCES

(1) M. S. Dresselhaus; G. Dresselhaus, P. C. Eklund, *Science of Fullerences and Carbon nanotubes* (Academic, San Diego, 1996).
(2) C. J. Brabec, A. Maiti, C. Roland, J. Bernholc, *Chem. Phys. Lett.*, **236**, 150-155 (1995).
(3) W. Deng, X. Xu, W. A. Goddard, *Nano Lett.* **12**, 2331 (2004).
(4) C. Bower, O. Zhou, W. Zhu, D. J. Werder, S. Jin, *Appl. Phys. Lett.* **77**, 2767 (2000).
(5) Y. Zhang, Y. Li, W. Kim, D. Wang, H. Dai, *Appl. Phys A* **74**, 325, (2002).
(6) Y. Li, J. Liu, Y. Q. Wang, Z. L. Wang, *Chem. Mater.* **13**, 1008 (2001).
(7) P. Nikolaev *et al*, *Chem. Phys. Lett.* **313**, 91 (1999).
(8) H. Cui, X. Yang, M. L. Simpson, D. H. Lowndes, M. Varela, *Appl. Phys. Lett.* **84**, 4077 (2004).
(9) P. E. Anderson, N. M. Rodriguez, *Chem. Mater.* **12**, 823 (2000).
(10) J. H. Hafner *et al*, *Chem. Phys. Lett.* **296**, 195-202 (1998).
(11) R. B. Little, *J. Cluster. Sci.* **14,** 135-185 (2003).
(12) M. S. Dresselhaus, G. Dresselhaus, P. H. Avouris, *Carbon Nanotubes* (Springer, Berlin, 2001).
(13) B. Liu *et al*, *J. Mater. Chem.* **11**, 2523 (2001).
(14) K. P. Loh, M. Lin, M. Yeadon, C. Boothroyd, Z. Hu, *Chem. Phys. Lett.* **387**, 40 (2004).
(15) Y. Li, W. Kim, Y. Zhang, M. Rolandi, D. Wang, H. Dai, J. Phys. Chem B **105**, 11424 (2001).
(16) J. Kong, A. M. Cassell, H. Dai, *Chem. Phys. Lett.* **292**, 567 (1998); J. Kong, H. Soh; A. M. Cassell; C. F. Quate, H. Dai, *Nature* **395**, 878, (1998).
(17) P. K. De Bokx, A. J. H. M. Kock, E. Boellaard, W. Klop, J. W.Geus, J. Catal. 96, 454 (1985).
(18) R. T. K. Baker, Carbon 27, 315 (1989).
(19) J. Tersoff , R. M. Tromp, *Phys. Rev. Lett.* **70**, 2782 (1993).
(20) P. Nikolaev *et al*, *Chem. Phys. Lett.* **313**, 91 (1999).
(21) M. Lin, J. P. Y. Tan, C. B. Boothroyd, K. P. Loh, E. S. Tok and Y. L. Foo, Nano Lett. 6, 449 (2006).